DMD Fast Forward. Published on April 4, 2006 as doi:10.1124/dmd.105.008870

DMD #8870

Expression, Purification and Characterization of Mouse Cyp2d22

Ai-Ming Yu and Robert L. Haining

Department of Basic Pharmaceutical Sciences, West Virginia University, Morgantown, WV 26506 (A-M. Y., R. L. H.)

Department of Pharmaceutical Sciences, University at Buffalo, State University of New York, Buffalo, NY 14260 (A.Y.)

DMD #8870

Running title: Characterization of Mouse Cyp2d22

Corresponding Author: Robert L. Haining, Ph. D

Department of Basic Pharmaceutical Sciences

School of Pharmacy

West Virginia University

PO Box 9530

Morgantown, WV 26506-9530

Tel: (304) 293-1450

Fax: (304) 293-2576

Email: rhaining@hsc.wvu.edu

Text pages: 20

Tables: 2

Figures: 2

References: 61

Words in Abstract: 233

Introduction: 558

Discussion: 818

Non-standard abbreviations used:

CYP: cytochrome P450; HT: hexahistidine-tagged; ES/LC-MS: electrospray ionization/liquid chromatography mass spectrometry; PMSF: phenylmethylsulfonyl fluoride; CHAPS: 3-[(3-cholamidopropyl)dimethyl-ammonio]-1-propanesulfonate; EDDP: 2-ethylidene-1,5-dimethyl-3,3-diphenylpyrrolidine; TFA: trifluoroacetic acid

Abstract

Metabolism of the prototype human CYP2D6 substrates, debrisoquine and bufuralol, proceeds at a much slower rate in mice, therefore the mouse has been proposed as an animal model for the human CYP2D6 genetic deficiency. To interpret the molecular mechanism of this deficiency, a cDNA belonging to the *CYP2D* gene subfamily, Cyp2d22 has been cloned and sequenced from a mouse mammary tumor derived cell line. In the current study, Cyp2d22 enzyme was over-expressed and purified from insect cells using a baculovirus-mediated system. The activity of this purified enzyme was directly compared with purified human CYP2D6 toward codeine, dextromethorphan, and methadone as substrates. Purified Cyp2d22 was found to catalyze the *O*-demethylation of dextromethorphan with significantly higher K_m values (250 μM) than that (4.2 μM) exhibited by purified human CYP2D6. The K_m for dextromethorphan *N*-demethylation by Cyp2d22 was found to be 418 μM, much lower than that observed with human CYP2D6 and near the K_m for dextromethorphan *N*-demethylation catalyzed by CYP3A4. CYP2D6 catalyzed codeine *O*-demethylation whereas Cyp2d22 and CYP3A4 mediated codeine *N*-demethylation. Furthermore methadone, a known CYP3A4 substrate and CYP2D6 inhibitor, was *N*-demethylated by Cyp2d22 with a K_m of 517 μM and V_{max} of 4.9 pmol/pmol/min. Quinidine and ketoconazole, potent inhibitors to CYP2D6 and CYP3A4 respectively, did not show strong inhibition toward Cyp2d22-mediated dextromethorphan *O*- or *N*-demethylation. These results suggest that mouse Cyp2d22 has its own substrate specificity beyond CYP2D6-like deficient activity.

Introduction

The superfamily of cytochrome P450 (*CYP*) genes encodes a large number of structurally similar, heme-containing monoxygenases which are found in virtually all living organisms, from bacteria to yeast, fungi, plants, mammals, and humans. In mammals and humans, CYP enzymes are mostly expressed in hepatic tissues and catalyze the oxidative metabolism of a wide variety of xenobiotics (Ortiz de Montellano, 1995). Many CYP isoforms are also expressed in extra-hepatic tissues, such as the skin, lung, kidney, breast, nasal mucosa, and brain (Peters et al., 1989; Amet et al., 1997; Gilham et al., 1997; Hedlund et al., 1998; Wolkenstein et al., 1998; Voirol et al., 2000; Siegle et al., 2001). These are increasingly understood to play an important role in the biosynthesis and biodegradation of endogenous compounds in addition to the biotransformation of xenobiotics, an area of active investigation in many laboratories.

CYP2D6 is a polymorphic human CYP isoform involved in the metabolism of about 25% of all prescribed drugs, including antiarrhythmics, antihypertensives, β-blockers, antipsychotics, and tricyclic antidepressants (Gonzalez et al., 1988; Skoda et al., 1988; Gonzalez and Idle, 1994; Nebert, 1997). CYP2D6 has also been shown to metabolize carcinogens and neurotoxins such as 1-methyl-4-phenyl-1,2,3,6-tetrahydropyridine (MPTP) (Fonne et al., 1987; Gilham et al., 1997; Nebert, 1997), 1,2,3,4-tetrahydroquinoline (Ohta et al., 1990) and indolealkylamines (Yu et al., 2003). A functional deficit of CYP2D6 activity is observed among up to 10% of Caucasians, who are termed as poor metabolizers compared with extensive metabolizers with normal activity. In addition to the pharmacokinetic clinical implications, poor metabolizers appear more likely to develop neurodegenerative disorders such as Alzheimer's or

Parkinson's disease (Saitoh et al., 1995; McCann et al., 1997). Mouse and dark agouti (DA) strain rat have been proposed as an animal models for this human CYP2D6 genetic deficiency since they also have an impaired ability to metabolize CYP2D6 probe drugs such as debrisoquine and bufuralol (Al-Dabbagh et al., 1981; Kahn et al., 1985; Gonzalez et al., 1987; Masubuchi et al., 1997), although some discrepancy is recognized from enzyme kinetics and gene analysis (Matsunaga et al., 1989; Adams et al., 1991; Barham et al., 1994). A Cyp2d enzyme partially purified from mouse liver microsomes does not exhibit debrisoquine 4-hydroxylase activity (Masubuchi et al., 1997). Recently, a cDNA belonging to the *Cyp2d* gene subfamily, termed Cyp2d22, was cloned and sequenced from a mouse mammary tumor derived cell line (Blume et al., 2000). This Cyp2d22 enzyme has identical amino acid sequence as that of the partially purified Cyp2d enzyme sequenced at the *N*-terminus (Masubuchi et al., 1997). Immunoblot analysis of mouse tissues with highly specific anti-Cyp2d22 antisera indicates that Cyp2d22 protein is most abundant in mouse liver, and also present in adrenal, ovary and mammary glands at intermediate levels (Blume et al., 2000).

The aim of the current study was to understand the enzymatic function of Cyp2d22 isoform, and contribute to interpretation of the molecular mechanism for CYP2D6 deficiency phenotype in mouse species. Cyp2d22 enzyme was over-expressed in insect cells using a baculovirus-mediated system, purified with affinity chromatography, and its whole molecular weight was determined by ESI/LC-MS analysis. Kinetic analyses with multiple substrates and inhibitors were performed for recombinant Cyp2d22 and compared with human CYP2D6 and CYP3A4. The results indicated that this murine Cyp2d22 enzyme, while possessing a deficit of CYP2D6-like

substrate specificity, has its intrinsic substrate specificity and enzymatic activities are rather similar to human CYP3A4.

Methods

Chemicals Dextromethorphan, dextrorphan, 3-methoxymorphinan, 3-hydroxymorphinan, fluoxetine and norfluoxetine standard samples were purchased from Research Biochemicals International (Natick, MA). Codeine, norcodeine, morphine, methadone, 2-ethylidene-1,5-dimethyl-3,3-diphenylpyrrolidine (EDDP), 2-mercaptoethanol, imidazole, reduced nicotinamide adenine dinucleotide phosphate (NADPH), L-α-dilauroylphosphatidylcholine (DLPC), phenylmethylsulfonyl fluoride (PMSF), and 60% perchloric acid were purchased from Sigma (St. Louis, MO). Testosterone and 6β-testosterone were from Steraloids (Newport, RI). 3-[(3-cholamidopropyl)dimethyl-ammonio]-1-propanesulfonate (CHAPS) was bought from Pierce (Rockford, IL). Ni-NTA Superflow was purchased from Qiagen (Valencia, CA). Emulgen 911 was from Kao-Atlas (Tokyo, Japan). HPLC solvents and other chemicals were of the highest grade commercially available and were used as received.

Molecular Biology CYP3A4 enzyme along with CYP reductase and cytochrome b5, expressed in BTI-TN-5B1-4 insect cells using baculovirus system, and the control insect cells infected with wide-type virus were purchased from BD Gentest (Woburn, MA), as well as the control insect cells infected with wide-type virus. Restriction enzymes were

bought from Boehringer-Mannheim, GibcoBRL, or New England Biolabs and were used in buffer systems provided by the manufacturers. High-Five *Trichoplusia ni* (*T. ni*) cells were obtained from InVitroGen (Carlsbad, CA). HyQCCM-3 media and fetal bovine serum (FBS) were from HyClone Laboratories (Logan, UT). General molecular biology methods were performed by standard procedures (Sambrook et al., 1989), and routine insect cell culture methods were followed as described by O'Reilly et al. (O'Reilly et al., 1994).

Cyp2d22 and CYP2D6 cDNAs were subcloned into pIZT/V5-His vector in order to introduce an *N*-terminal hexahistidine tag. DNA sequences were confirmed by complete gene sequencing using an Applied Biosystems ABI-Prism 377 and Perkin-Elmer ABI BigDye™ Terminator cycle sequencing kit. These cDNA were transferred from pIZT/V5-His into pFastBac/HT vector (Life Technologies, www.lifetech.com) using similar digestion procedures for creation of recombinant baculovirus.

Protein Expression and Purification Rat NADPH cytochrome P450 reductase was expressed and purified from bacterial cultures according to published procedures (Shen et al., 1991). Spectral CYP activity was determined by the method of Omura and Sato (Omura and Sato, 1964) and was used as a mean to establish optimal conditions for CYP expression and purification. Expression, purification and biomedical characterization of unmodified CYP2D6 enzyme was reported elsewhere (Yu et al., 2001; Yu et al., 2002). Baculovirus-mediated HT-Cyp2d22 and HT-CYP2D6 were over-expressed in *T. ni* suspension cultures using a baculovirus expression system as CYP2C9 (Haining et al., 1996; Yu et al., 2001), and purified using affinity column chromatography. All

purification steps were carried out at 4^0C, and all buffers were at pH 7.4. The crude insect cell pellet was homogenized in solubilization buffer [20% (v/v) glycerol, 1mM PMSF, 1% (v/v) Emulgen 911 and 20 mM 2-mercaptoethanol in 50 mM potassium phosphate buffer] by making 5-10 passes with a glass/Teflon homogenizer. CYP isoform was solubilized by stirring the homogenized insect cell pellet for 60 min, and the insoluble material was removed by centrifugation at 100,000 g for 60 min. The supernatant was loaded onto a Ni-NTA Superflow column (1 mL per 20 nmols of CYP) pre-equilibrated with solubilization buffer at 30 mL/h. After the sample was loaded, the column was washed with 4 columns of wash buffer A (0.5 M sodium chloride in solubilization buffer) at 30 mL/h. Then the column was washed overnight with wash buffer B [20% (v/v) glycerol, 1 mM PMSF, 2 mM CHAPS, 0.5 M sodium chloride, 5 mM imidazole and 20 mM 2-mercaptoethanol in 50 mM potassium phosphate buffer]. The column was further washed with four columns of wash buffer C (25 mM imidazole in wash buffer B), followed by the elution with 100 mM imidazole in wash buffer B. The fractions containing CYP enzyme were combined, and dialyzed overnight against buffer D [20% (v/v) glycerol and 0.1 mM EDTA in 100 mM potassium phosphate buffer). Purified hexahistidine tagged P450 isoform was aliquoted and stored at -80^0C until further use. Purity is estimated at greater than 95% as estimated by SDS-PAGE followed by staining with Coomassie blue (Figure 1).

ESI/LC-MS Analysis of Purified Proteins ESI/LC-MS analyses were performed on a Micromass Quattro II tandem quadrupole mass spectrometer (Micromass Ltd., Manchester, UK) coupled to an HPLC [Shimadzu LC-10AD with SPD-10AV UV-vis

variable detector (Shimadzu Scientific Instruments, Inc., Columbia, MD)]. The instrument was controlled by a computer running Windows NT based Micromass MassLynxNT® 3.2 software. The source temperature was 150^{0}C with the cone voltage set to 55 kV. Solvent flow through the POROS R2 perfusion column (2.1×150 mm) from Perseptive Biosystems (Cambridge, MA) was 0.2 mL/min with 100% of the flow (50 pmol of protein injected) being diverted to the mass spectrometer. Acquisition was carried out from m/z 500-2000 Da in the CONTIUUM scanning mode. ESI mass spectra were collected, the individual scans across the HPLC peak were combined, and each spectrum was deconvoluted using the MaxEnt® program.

Assay of Enzymatic Activity CYP enzymes were reconstituted with rat cytochrome P450 reductase (1:2 ratio) and with dilauroylphosphatidylcholine as described (Yu et al., 2001) prior to the addition of substrate. All reactions were carried out at 37^{0}C in 100 mM potassium phosphate, pH 7.4, in a final volume of 200 μL. Reactions were optimized for protein and time with respect to linearity prior to kinetic analysis. Reactions were initiated by the addition of 20 μL of 10 mM NADPH after 5 min pre-incubation with the substrate at 37^{0}C. For the kinetic analyses, dextromethorphan concentrations in the incubations were 1-50 μM for (non)HT-CYP2D6-mediated *O*-demethylation, 0.5-8 mM for (non)HT-CYP2D6-catalzyed *N*-demethylation, and 25-3000 μM for HT-Cyp2d22- and CYP3A4-catalyzed *O*- and *N*-demethylation. Codeine concentrations were 50-3000 μM for investigation of its *O*-demethylation and 0.2-8 mM for *N*-demethylation. Final fluoxetine concentrations in the reactions were 0.5-50 μM for (non)HT-CYP2D6 and 10-250 μM for HT-Cyp2d22 and CYP3A4. Methadone final concentrations in the

DMD Fast Forward. Published on April 4, 2006 as DOI: 10.1124/dmd.105.008870
This article has not been copyedited and formatted. The final version may differ from this version.

incubations were 10-1000 μM for examination the *N*-demethylation. Testosterone concentration was fixed at 50 or 250 μM to investigate whether Cyp2d22 catalyzes its hydroxylations. Same concentrations of testosterone were used for the control reactions with CYP2D6 and CYP3A4. Negative control incubations for all the studies included reactions without the addition of reductase, CYP isozyme, substrate or NADPH. For inhibition studies, dextromethorphan concentration was fixed at 1 μM (for *O*-demethylation) and 1 mM (*N*-demethylation), and quinidine and ketoconazole concentrations ranged from 5-10,000 nM and 10-3000 nM, respectively. To determine the Ki value for quinidine against HT-CYP2D6 activity, three different concentrations were used for dextromethorphan (1, 3, and 10 μM) and five different concentrations for quinidine (0, 5, 10, 50 and 100 nM). All reactions were carried out in duplicate. After 5-10 min incubation, the reactions were terminated with 10 μL of 70% perchloric acid except the reactions with testosterone and methadone, which were stopped with 200 μL of ice-cold acetonitrile. The mixture was vortexed for 20 s, cooled on ice for 10 min, and centrifuged at 14,000 g for 10 min. The supernatant was transferred to new vial, and directly injected for HPLC or LC-MS analysis.

HPLC and LC-MS Quantification of Metabolites HPLC analyses were carried out on a Waters Alliance system consisting of the 2690 separation module, the 2487 dual λ absorbance detector and the 474 scanning fluorescence detector controlled with Millennium[32] software. A 4.6×250 mm Spherisob® 5 μM phenyl analytical column (Waters, USA) was used to separate dextromethorphan, codeine, fluoxetine, methadone and their metabolites. A 150×4.6 mm ID Nucleosil C18 column (Supelco, USA) was

used to analyze testosterone and its metabolites. Analysis of dextromethorphan and its metabolites was performed essentially as described (Yu and Haining, 2001). Dextromethorphan and its metabolites, 3-methoxymorphinan, and dextrorphan were eluted at 13.6, 10.7, and 8.36 min respectively. HPLC analyses of fluoxetine and norfluoxetine, codeine and its metabolites, methadone and its metabolites, and testosterone and 6β-hydroxytestosterone were carried out according to these published methods (Venn and Michalkiewicz, 1990; Pierce et al., 1992; Norman et al., 1993; Purdon and Lehman-McKeeman, 1997) with some modifications. Generally, separation of fluoxetine and its metabolites was achieved with a mobile phase containing 60% Buffer E (10 mM potassium phosphate monobasic, pH=3.5 adjusted with orthophosphoric acid) and 40% acetonitrile. The excitation and emission wavelengths of the fluorescence detector were set at 235 and 310 nm respectively. Fluoxetine and its *N*-demethylated metabolite, norfluoxetine, were eluted at 14.1 min and 11.9 min. A mobile phase consisted of 65% water with 0.1% TFA, and 35% acetonitrile and water mixture (400/600, V/V) was used to separate codeine and its metabolites norcodeine and morphine, which were eluted at 15.8, 9.2 and 8.2 min. The excitation and emission wavelengths of the fluorescence detector were set at 280 and 335 nm respectively for the analysis of codeine and its metabolites. Methadone and its metabolites were separated with a mobile phase containing with 30% buffer E and 70% acetonitrile, and detected with the UV detector set at 210 nm. Methadone and EDDP were eluted at 13.6 min and 16.7 min respectively. Gradient elution (50%-80% methanol in water from 0-10 min) was used to separate testosterone and its metabolites, which were detected using UV detector

with a wavelength set at 240 nm. 6β-Hydroxytestosterone and testosterone were eluted at 5.16 min and 8.88 min, respectively.

ESI/LC-MS analyses were used to quantify EDDP produced from methadone , which were performed by using a Micromass ZMD 4000 quadrupole mass spectrometer (Waters Micromass, USA) coupled to a Waters Alliance HPLC System. The instrument was controlled by a computer running Windows NT based Micromass MasslynxNT® V3.5 software. The optimized instrument parameters were as follow: source temperature 100^0C, cone voltage 29 kV. Isocratic elution with 30% water containing 0.1% TFA and 70% acetonitrile was used to separate the metabolite and substrate. Solvent flow through the Spherisob® phenyl analytical column was 1.0 mL/min with 35% of the flow being diverted to the mass spectrometer. Raw data were collected in the SIR mode with m/z set to 278Da.

Data Analysis Enzyme Michaelis-Menten parameters, K_m and V_{max}, were estimated by nonlinear regression (GraphPad Prizm™ 3.02). Linear regression analyses were conducted using Microsoft Excel 2000.

Results

Expression and purification of HT-Cyp2d22 and HT-CYP2D6 enzymes

High titer baculovirus stocks, *T. ni* suspension culture, and heme addition proceeded in a manner analogous to that used for CYP2C9 and CYP2D6 (Haining et al., 1996; Yu et al., 2001). Cultures exhibiting greater than 100 nmol/liter equivalents of

active P450 enzyme were used for purification. Holoprotein yields were estimated by measuring carbon monoxide difference spectra. Both HT-Cyp2d22 and HT-CYP2D6 enzymes behaved in a chromatographically identical manner throughout the purification procedures. Contaminants were removed by passage through nickel resin. Highly purified, detergent free CYP enzyme was collected after dialysis the fractions eluted from the column (Fig. 1). The total yields were 61.1% and 55.7% for HT-Cyp2d22 and HT-CYP2D6 enzymes, respectively. The carbon monoxide difference spectra for HT-Cyp2d22 isoform exhibited Soret maxima at 449 nm with no evidence of cytochrome P420 formation (Fig. 2). Meanwhile, all these samples were analyzed by Western blotting using an anti-CYP2D6 antibody. As expected, all CYP2D protein products were detected in these samples although the antibody is a polypeptide specific to CYP2D6 isoform (data not shown).

ESI/LC-MS analysis of HT-Cyp2d22 and HT-CYP2D6 isoforms

We were able to determine the whole molecular weight of each purified CYP enzyme using ESI/LC-MS analysis in order to compare with their theoretical molecular weights. The experimental molecular weights were 60287.5 da and 59430.0 da for HT-Cyp2d22 and HT-CYP2D6 isoform, respectively, compared to the molecular weight values of 60222.6 da and 59384.3 da calculated according to their amino acid sequences. The differences between the experimental and predicted molecular weights were only 64.9 da and 45.7 da for HT-Cyp2d22 and HT-CYP2D6 proteins, suggesting that these proteins expressed in insect cells do not have any post-translational modification, and such modification is unnecessary for their CYP activity.

DMD Fast Forward. Published on April 4, 2006 as DOI: 10.1124/dmd.105.008870
This article has not been copyedited and formatted. The final version may differ from this version.

Dextromethorphan O- and N-demethylation

Dextromethorphan, an over-the-counter antitussive drug, is a widely used probe for polymorphic CYP2D6 activity both *in vivo* and *in vitro*, and possibly for CYP3A activity (Gorski et al., 1994; Ducharme et al., 1996; Jones et al., 1996; Krecic-Shepard et al., 1999; Yu and Haining, 2001). CYP2D6 catalyzes both dextromethorphan *O*- and *N*-demethylation, with a low and a high K_m, respectively (Yu et al., 2001), suggesting CYP2D6 enzyme may also contain two substrate orientations or two active sites. Polyhistidine-tagged CYP2D6 also carried out these two reactions with two similar K_m values, 4.2 μM and 4.8 mM, compared to 5.1 μM and 3.9 mM by non-polyhistidine-tagged CYP2D6 (Table 1), indicating the addition of hexahistidine tag at the *N*-terminal did not affect the drug-metabolizing activity of CYP2D6.

Dextromethorphan was then used to compare the difference in enzymatic activity between mouse Cyp2d22 and human CYP2D6 isoforms. To our surprise, dextromethorphan *N*-demethylation was the main pathway catalyzed by HT-Cyp2d22, while *O*-demethylation was the main metabolic pathway mediated by (non)HT-CYP2D6 at comparably low substrate concentration (100-200 μM). The calculated apparent constant value for dextromethorphan *O*-demethylation catalyzed by HT-Cyp2d22 was 250 μM, much higher than that by HT-CYP2D6 (Table 1). However, HT-Cyp2d22 catalyzed dextromethorphan *N*-demethylation with a K_m value of 418 μM, much lower than the K_m value of 4750 μM by HT-CYP2D6. Since dextromethorphan *N*-demethylation is known as CYP3A4-mediated biotransformation pathway, the catalytic activity of this reaction was compared between mouse Cyp2d22 and human CYP3A4. Interestingly, their apparent constant and intrinsic clearance values were very close,

which were 418 μM and 48.7 nL/pmol P450/min for HT-Cyp2d22; 302 μM and 81.1 nL/pmol P450/min for CYP3A4. We also detected the *O*-demethylated metabolites, dextrorphan, produced by Cyp2d22 and CYP3A4 isoforms, and compared the kinetic parameters between them. Again, their apparent constant and intrinsic clearance values for dextromethorphan *O*-demethylation were very close, which were 171 μM and 32.5 nL/pmol P450/min for HT-Cyp2d22, and 157 μM and 34.3 nL/pmol P450/min for CYP3A4 (Table 1). Since this similarity in catalytic activity between mouse Cyp2d22 and human CYP3A4 isoforms were not expected, more substrates were selected to further compare the similarity in enzymatic activities between them.

Codeine O- and N-demethylation

Codeine, whose backbone chemical structure is strikingly similar to that of dextromethorphan, is metabolized to morphine and norcodeine through *O*- and *N*-demethylation respectively. In humans, codeine *O*- and *N*-demethylation are attributable to isoforms CYP2D6 and CYP3A, respectively (Caraco et al., 1996; Yue and Sawe, 1997). In our previous study on CYP2D6 pharmacogenetics, we found that all CYP2D6 allelic variants catalyzed primarily codeine *O*-demethylation (Yu et al., 2002).

Morphine was produced by HT-CYP2D6 with a K_m at 277 μM, which was close to that (178 μM) by unmodified CYP2D6 isoform. Norcodeine was not detected in the incubations with (non)-HT-CYP2D6 enzyme. However, morphine was not detected in the incubation reactions containing HT-Cyp2d22 or CYP3A4, and norcodeine was produced as the only metabolite. The V_{max} and K_m values for codeine *N*-demethylation catalyzed by HT-Cyp2d22 were 3.8 pmol/pmol P450/min, and 2150 μM, respectively. CYP3A4

proceeded codeine *N*-demethylation with a K_m of 619 μM (Table 2), which was only about 3-fold lower than that by HT-Cyp2d22.

Fluoxetine and methadone N-demethylation

Fluoxetine is a well-known potent inhibitor of CYP2D6as well as a substrate, which is *N*-demethylated to form norfluoxetine in humans. HT-Cyp2d22 catalyzed fluoxetine *N*-demethylation with an estimated K_m value of 110 μM, much higher than the K_m value of 2.5 μM and 6.6 μM mediated by HT-CYP2D6 and non-HT-CYP2D6, respectively, but yet close to the K_m value of 168μM exhibited by CYP3A4 (Table 2).

Methadone, also a potent inhibitor to CYP2D6, is *N*-demethylated by CYP3A4 to produce EDDP in humans (Iribarne et al., 1996; Moody et al., 1997; Oda and Kharasch, 2001). Unexpectedly, purified HT-Cyp2d22 also catalyzed this biotransformation reaction. The calculated apparent constant value of methadone *N*-demethylation by HT-Cyp2d22 was 517 μM, much higher than the K_m value of 32.9 μM mediated by CYP3A4 (Table 2).

Testosterone 6β-Hydroxylation

Steroid hydroxylation is a well-established function of human CYP3A and murine Cyp2d isoforms. Testosterone 6β-hydroxylation, a widely used index reaction for CYP3A4 activity, was reported to be catalyzed by the partially purified mouse Cyp2d enzyme (Masubuchi et al., 1997), but not mediated by *Cyp2d22*-transfected cells (Blume et al., 2000). We believe this partially purified mouse Cyp2d enzyme was the Cyp2d22 isoform because its reported amino acid sequence at the *N*-terminus was exactly the same

as that of Cyp2d2 protein, and different from that of any other known murine Cyp2d isoforms. To clarify this literature discrepancy and to further compare the substrate specificity between mouse Cyp2d22 and human CYP3A4, we examined whether the purified HT-Cyp2d22 could also catalyze testosterone 6β-hydroxylation reaction. As expected, 6β-hydroxytestosterone was detected in the incubation reactions with human CYP3A4, but not in the reactions with (non)-HT-CYP2D6. Meanwhile, HT-Cyp2d22 did not mediate testosterone 6β-hydroxylation, which was consistent with the result obtained by Blume (Blume et al., 2000).

Inhibition Analysis

CYP2D6 and CYP3A4 inhibitors were utilized to study and compare their inhibition potencies against the Cyp2d22 isoform. The mean K_i value of quinidine for dextromethorphan *O*-demethylation catalyzed by purified CYP2D6 enzyme was determined as 34 nM (Yu and Haining, 2001). Using HT-CYP2D6, the mean K_i value obtained for the dextromethorphan *O*-demethylation was 68 nM, indicating that the inhibition potency of quinidine to CYP2D6 enzymatic activity was not affected by the fusion of the hexahistidine tag. However, quinidine (5-500 nM) did not show strong inhibition (≤ 20%) to HT-Cyp2d22-catalyzed dextromethorphan *O*- or *N*-demethylation. Rather, a well-known CYP3A4 inhibitor ketoconazole (100-300 nM) showed moderate inhibition (20-40%) against Cyp2d22-catalyzed dextromethorphan *N*- and *O*-demethylation (not shown).

Sequence Similarity of Cyp2d22 to Human CYP2D6 and CYP3A4

The predicted mouse Cyp2d22 protein consists of 505 amino acids, and shares 74% amino acid sequence identity with human CYP2D6, a little greater than that with other known murine Cyp2d isoforms (69%, 69%, and 67% for Cyp2d9, Cyp2d10, and Cyp2d11, respectively). Since the mouse Cyp2d22 enzyme showed certain enzymatic similarity as human CYP3A4, we then compared its sequence similarity to CYP3A4. As expected, the amino acid sequence of Cyp2d22 was less than 40% identical to CYP3A4. Nonetheless, the amino acid sequence of essential components such as the cysteine-pocket, heme-binding domain with meander, and I, J helix were highly conserved among all isoforms examined.

Discussion

At least twenty *CYP2D* genes have now been identified in mammals and humans (Kimura et al., 1989; Nelson et al., 1996; Mankowski et al., 1999; Blume et al., 2000; Hosseinpour and Wikvall, 2000). In humans, three *CYP* genes belonging to the *CYP2D* subfamily *CYP2D6*, *CYP2D7P* and *CYP2D8P*, have been identified. However, *CYP2D7P* and *CYP2D8P* which present typically in a given haplotype are pseudogenes, and only *CYP2D6* produces functional protein in human liver (Kimura et al., 1989). *CYP2D1* through *CYP2D5*, and *CYP2D18* are found in the rat, and *Cyp2d9* through *Cyp2d13*, and *Cyp2d22* are from the mouse (Nelson et al., 1996; Blume et al., 2000). The mouse *Cyp2d22* gene contains 1515 base pairs and encodes a protein with 505 amino acids. Its DNA sequence shares 87-90% identity with rat *CYP2D3* through *CYP2D5* and *CYP2D18*, with a corresponding amino acid identity of 71-85%. Interestingly, the amino

acid sequence of the predicted mouse Cyp2d22 is less similar to mouse Cyp2d9 (69%), Cyp2d10 (69%), or Cyp2d11 (67%) than human CYP2D6 (74%), and monkey CYP2D17 (75%; 43).

Most of these mammalian CYP2D enzymes are expressed in liver and are known to be responsible for the biotransformation of xenobiotics. Given the sequence similarity with CYP2D6, we reasoned that characterization of the enzymatic function for the encoded Cyp2d22 protein would contribute to the understanding of the CYP2D6-like phenotype or lack thereof in mice. Recently, Lofgren et al. reported CYP2D6-like enzymatic activity in mouse liver microsomes. This activity correlated with a protein which was immunoreactive to anti-rat Cyp2d4 antibody and which appeared more prevalent in females than males (Lofgren et al., 2004). Cyp2d22 however is known to be highly expressed in both male and female mouse liver, and is modestly expressed in a variety of other tissues, such as adrenal, ovary, and mammary glands (Blume et al., 2000). Thus our results would suggest that Cyp2d22 is *not* the CYP2D isozyme responsible for the CYP2D6-like enzyme activity reported by Lofgren in female mouse liver (Lofgren et al., 2004).

Mouse Cyp2d22, purified from cDNA-transfected insect cells and characterized by immunochemical and ESI/LC-MS analyses, indeed catalyzes the biotransformation of dextromethorphan, and shows substantially decreased *O*-demethylase activity as compared to human CYP2D6 (Table 1). However, Cyp2d22 produces more *N*-demethylated metabolite, 3-methoxymorphinan, than *O*-demethylated metabolite, dextrorphan. The switch of the metabolic pathways of dextromethorphan metabolism suggests a difference of its enzymatic function from that of CYP2D6. Moreover,

Cyp2d22 catalyzes dextromethorphan *N*-demethylation with much K_m value than CYP2D6, but similar to that exhibited by CYP3A4 (Table 1). The functional similarity between Cyp2d22 and CYP3A4 is further confirmed by the results obtained from codeine, fluoxetine and methadone biotransformation reactions (Table 2) although the identity of amino acid sequence is less than 40% between these isoforms. This similarity in substrate specificity between CYP isoforms across the families and species may provide some helpful information for the study of CYP orthogenesis. Nevertheless, it remains to be determined whether the enzymatic functions of mouse Cyp2d22 *in vivo* are largely similar to those of human CYP3A4.

Distinct enzymatic function between Cyp2d22 and CYP2D6 is presumably due to their own unique active sites distinct from each other. This is supported by our inhibition study which shows that quinidine strongly inhibits CYP2D6-mediated drug metabolism whereas does not reduce Cyp2d22 enzymatic activity. In contrast, CYP3A4 selective inhibitor, ketoconazole, shows modest inhibition again Cyp2d22 activity. Knowledge of selective and potent inhibitors of the Cyp2d22 isoform could be of great benefit to future functional and molecular modeling studies involving the Cyp2d22 and other murine Cyp2d enzymes.

The presence of CYP2D isoforms in extrahepatic tissues, such as CYP2D6 and CYP2D18 in human and rat brains, respectively (Kawashima et al., 1996; Gilham et al., 1997; Voirol et al., 2000; Siegle et al., 2001), has been demonstrated, where they may be involved in the biosynthesis and biodegradation of endogenous compounds. Indeed, CYP2D6 has been shown to mediate the catabolism of phenylalkylamines (Hiroi et al., 1998; Haining and Yu, 2003) and indolealkylamines (Yu et al., 2003). CYP2D18, which

shares 85% amino acid sequence identity with Cyp2d22 has also been shown to catalyze dopamine oxidation (Thompson et al., 2000). CYP2D25, purified from pig liver, has demonstrated vitamin D3 25-hydroxylase activity with an apparent K_m of 0.1 μM, a concentration within the physiological range (Hosseinpour and Wikvall, 2000). No evidence indicates that Cyp2d22 metabolizes endogenous steroids of any kind (Blume et al., 2000). However, the partially purified mouse Cyp2d enzyme, which should be the Cyp2d22 protein according to the reported amino acid sequence, catalyzes a variety of testosterone hydroxylation reactions (Masubuchi et al., 1997). Our experiments reveal that neither Cyp2d22 nor CYP2D6 produce any hydroxylated metabolite from testosterone whereas CYP3A4 does. This result is consistent with that reported by Blume (Blume et al., 2000) using *Cyp2d22*-transfected cells. In fact, no recombinant mouse or rat CYP2D isoforms have been found to catalyze the reaction to date. Nonetheless, further studies will be required to investigate whether murine Cyp2d isozyme catalyzes the biotransformation of endogenous compounds such as the neuroregulatory monoamines.

In summary, biochemical characterization, ESI/LC-MS analysis and immunochemical confirmation of the mouse Cyp2d22 isozyme was achieved, following the purification from insect cells utilizing a baculovirus-mediated expression system. Comparative kinetic analyses toward multiple substrate reactions and inhibition studies show that Cyp2d22 does possess deficient human CYP2D6-like activity, but has certain degree of similarity in enzymatic function as human CYP3A4. These results suggest that

murine Cyp2d22 has substrate specificity intrinsically different from other mammalian CYP2D isozymes.

References

Adams M, Lennard MS, Otton SV, Tucker GT and Woods HF (1991) Assessment of the mouse as an experimental model for studying polymorphic oxidation of the sparteine/debrisoquine type. *Biochem Pharmacol* **42:**947-949.

Al-Dabbagh SG, Idle JR and Smith RL (1981) Animal modelling of human polymorphic drug oxidation--the metabolism of debrisoquine and phenacetin in rat inbred strains. *J Pharm Pharmacol* **33:**161-164.

Amet Y, Berthou F, Fournier G, Dreano Y, Bardou L, Cledes J and Menez JF (1997) Cytochrome P450 4A and 2E1 expression in human kidney microsomes. *Biochem Pharmacol* **53:**765-771.

Barham HM, Lennard MS and Tucker GT (1994) An evaluation of cytochrome P450 isoform activities in the female dark agouti (DA) rat: relevance to its use as a model of the CYP2D6 poor metaboliser phenotype. *Biochem Pharmacol* **47:**1295-1307.

Blume N, Leonard J, Xu ZJ, Watanabe O, Remotti H and Fishman J (2000) Characterization of Cyp2d22, a novel cytochrome P450 expressed in mouse mammary cells. *Arch Biochem Biophys* **381:**191-204.

Caraco Y, Tateishi T, Guengerich FP and Wood AJ (1996) Microsomal codeine N-demethylation: cosegregation with cytochrome P4503A4 activity. *Drug Metab Dispos* **24:**761-764.

Ducharme J, Abdullah S and Wainer IW (1996) Dextromethorphan as an in vivo probe for the simultaneous determination of CYP2D6 and CYP3A activity. *J Chromatogr B Biomed Appl* **678:**113-128.

Fonne P-R, Bargetzi MJ and Meyer UA (1987) MPTP, the neurotoxin inducing Parkinson's disease, is a potent competitive inhibitor of human and rat cytochrome P450 isozymes (P450bufI, P450db1) catalyzing debrisoquine 4-hydroxylation. *Biochemical and Biophysical Research Communications* **148:**1144-1150.

Gilham DE, Cairns W, Paine MJ, Modi S, Poulsom R, Roberts GC and Wolf CR (1997) Metabolism of MPTP by cytochrome P4502D6 and the demonstration of 2D6 mRNA in human foetal and adult brain by in situ hybridization. *Xenobiotica* **27:**111-125.

Gonzalez FJ and Idle JR (1994) Pharmacogenetic phenotyping and genotyping. Present status and future potential. *Clin Pharmacokinet* **26:**59-70.

Gonzalez FJ, Matsunaga T, Nagata K, Meyer UA, Nebert DW, Pastewka J, Kozak CA, Gillette J, Gelboin HV and Hardwick JP (1987) Debrisoquine 4-hydroxylase: characterization of a new P450 gene subfamily, regulation, chromosomal mapping, and molecular analysis of the DA rat polymorphism. *DNA* **6:**149-161.

Gonzalez FJ, Skoda RC, Kimura S, Umeno M, Zanger UM, Nebert DW, Gelboin HV, Hardwick JP and Meyer UA (1988) Characterization of the common genetic defect in humans deficient in debrisoquine metabolism. *Nature* **331:**442-446.

Gorski JC, Jones DR, Wrighton SA and Hall SD (1994) Characterization of dextromethorphan N-demethylation by human liver microsomes. Contribution of the cytochrome P450 3A (CYP3A) subfamily. *Biochem Pharmacol* **48:**173-182.

Haining R and Yu A (2003) Cytochrome P450 Pharmacogenetics, in: *Cytochrome p450 and Drug Metabolism* (Lee J ed), pp 343-387, FontisMedia.

Haining RL, Hunter AP, Veronese ME, Trager WF and Rettie AE (1996) Allelic variants of human cytochrome P450 2C9: baculovirus-mediated expression, purification, structural characterization, substrate stereoselectivity, and prochiral selectivity of the wild-type and I359L mutant forms. *Archives of Biochemistry and Biophysics* **333:**447-458.

Hedlund E, Gustafsson JA and Warner M (1998) Cytochrome P450 in the brain: 2B or not 2B. *Trends Pharmacol Sci* **19:**82-85.

Hiroi T, Imaoka S and Funae Y (1998) Dopamine formation from tyramine by CYP2D6. *Biochem Biophys Res Commun* **249:**838-843.

Hosseinpour F and Wikvall K (2000) Porcine microsomal vitamin D(3) 25-hydroxylase (CYP2D25). Catalytic properties, tissue distribution, and comparison with human CYP2D6. *J Biol Chem* **275:**34650-34655.

Iribarne C, Berthou F, Baird S, Dreano Y, Picart D, Bail JP, Beaune P and Menez JF (1996) Involvement of cytochrome P450 3A4 enzyme in the N-demethylation of methadone in human liver microsomes. *Chem Res Toxicol* **9:**365-373.

Jones DR, Gorski JC, Haehner BD, O'Mara EM, Jr. and Hall SD (1996) Determination of cytochrome P450 3A4/5 activity in vivo with dextromethorphan N-demethylation. *Clin Pharmacol Ther* **60:**374-384.

Kahn GC, Rubenfield M, Davies DS, Murray S and Boobis AR (1985) Sex and strain differences in hepatic debrisoquine 4-hydroxylase activity of the rat. *Drug Metab Dispos* **13:**510-516.

Kawashima H, Sequeira DJ, Nelson DR and Strobel HW (1996) Genomic cloning and protein expression of a novel rat brain cytochrome P-450 CYP2D18* catalyzing imipramine N-demethylation. *J Biol Chem* **271:**28176-28180.

Kimura S, Umeno M, Skoda RC, Meyer UA and Gonzalez FJ (1989) The human debrisoquine 4-hydroxylase (CYP2D) locus: sequence and identification of the polymorphic CYP2D6 gene, a related gene, and a pseudogene. *Am J Hum Genet* **45:**889-904.

Krecic-Shepard ME, Barnas CR, Slimko J, Gorski JC, Wainer IW and Schwartz JB (1999) In vivo comparison of putative probes of CYP3A4/5 activity: erythromycin, dextromethorphan, and verapamil. *Clin Pharmacol Ther* **66:**40-50.

Lofgren S, Hagbjork AL, Ekman S, Fransson-Steen R and Terelius Y (2004) Metabolism of human cytochrome P450 marker substrates in mouse: a strain and gender comparison. *Xenobiotica* **34:**811-834.

Mankowski DC, Laddison KJ, Christopherson PA, Ekins S, Tweedie DJ and Lawton MP (1999) Molecular cloning, expression, and characterization of CYP2D17 from cynomolgus monkey liver. *Arch Biochem Biophys* **372:**189-196.

Masubuchi Y, Iwasa T, Hosokawa S, Suzuki T, Horie T, Imaoka S, Funae Y and Narimatsu S (1997) Selective deficiency of debrisoquine 4-hydroxylase activity in mouse liver microsomes. *J Pharmacol Exp Ther* **282:**1435-1441.

Matsunaga E, Zanger UM, Hardwick JP, Gelboin HV, Meyer UA and Gonzalez FJ (1989) The CYP2D gene subfamily: analysis of the molecular basis of the debrisoquine 4-hydroxylase deficiency in DA rats. *Biochemistry* **28:**7349-7355.

McCann SJ, Pond SM, James KM and Le Couteur DG (1997) The association between polymorphisms in the cytochrome P-450 2D6 gene and Parkinson's disease: a case-control study and meta-analysis. *J Neurol Sci* **153:**50-53.

Moody DE, Alburges ME, Parker RJ, Collins JM and Strong JM (1997) The involvement of cytochrome P450 3A4 in the N-demethylation of L-alpha-acetylmethadol (LAAM), norLAAM, and methadone. *Drug Metab Dispos* **25:**1347-1353.

Nebert DW (1997) Polymorphisms in drug-metabolizing enzymes: what is their clinical relevance and why do they exist? *Am J Hum Genet* **60:**265-271.

Nelson DR, Koymans L, Kamataki T, Stegeman JJ, Feyereisen R, Waxman DJ, Waterman MR, Gotoh O, Coon MJ, Estabrook RW, Gunsalus IC and Nebert DW (1996) P450 superfamily: update on new sequences, gene mapping, accession numbers and nomenclature. *Pharmacogenetics* **6:**1-42.

Norman TR, Gupta RK, Burrows GD, Parker G and Judd FK (1993) Relationship between antidepressant response and plasma concentrations of fluoxetine and norfluoxetine. *Int Clin Psychopharmacol* **8:**25-29.

Oda Y and Kharasch ED (2001) Metabolism of methadone and levo-alpha-acetylmethadol (LAAM) by human intestinal cytochrome P450 3A4 (CYP3A4): potential contribution of intestinal metabolism to presystemic clearance and bioactivation. *J Pharmacol Exp Ther* **298:**1021-1032.

Ohta S, Tachikawa O, Makino Y, Tasaki Y and Hirobe M (1990) Metabolism and brain accumulation of tetrahydroisoquinoline (TIQ) a possible parkinsonism inducing substance, in an animal model of a poor debrisoquine metabolizer. *Life Sci* **46:**599-605.

Omura T and Sato R (1964) The Carbon Monoxide-binding Pigment of Liver Microsomes I. Evidence for its Hemoprotein Nature. *J Biol Chem* **239:**2370-2378.

O'Reilly DR, Miller LK and Luckow VA (1994) *Baculovirus expression vectors - A laboratory manual*. Oxford University Press, Oxford, NY.

Ortiz de Montellano PR (1995) *Cytochrome P450: Structure, Mechanism, and Biochemistry*. Plenum Press, London.

Peters WH, Nagengast FM and van Tongeren JH (1989) Glutathione S-transferase, cytochrome P450, and uridine 5'-diphosphate-glucuronosyltransferase in human small intestine and liver. *Gastroenterology* **96:**783-789.

Pierce TL, Murray AG and Hope W (1992) Determination of methadone and its metabolites by high performance liquid chromatography following solid-phase extraction in rat plasma. *J Chromatogr Sci* **30:**443-447.

Purdon MP and Lehman-McKeeman LD (1997) Improved high-performance liquid chromatographic procedure for the separation and quantification of hydroxytestosterone metabolites. *J Pharmacol Toxicol Methods* **37:**67-73.

Saitoh T, Xia Y, Chen X, Masliah E, Galasko D, Shults C, Thal LJ, Hansen LA and Katzman R (1995) The CYP2D6B mutant allele is overrepresented in the Lewy body variant of Alzheimer's disease. *Ann Neurol* **37:**110-112.

Sambrook J, Fritsch EF and Maniatis T (1989) *Molecular Cloning: A Laboratory Manual*. Cold Spring Harbor Laboratory Press, Cold Spring Harbor, NY.

Shen AL, Christensen MJ and Kasper CB (1991) NADPH-cytochrome P-450 oxidoreductase. The role of cysteine 566 in catalysis and cofactor binding. *J Biol Chem* **266:**19976-19980.

Siegle I, Fritz P, Eckhardt K, Zanger UM and Eichelbaum M (2001) Cellular localization and regional distribution of CYP2D6 mRNA and protein expression in human brain. *Pharmacogenetics* **11:**237-245.

Skoda RC, Gonzalez FJ, Demierre A and Meyer UA (1988) Two mutant alleles of the human cytochrome P-450db1 gene (P450C2D1) associated with genetically deficient metabolism of debrisoquine and other drugs. *Proc Natl Acad Sci U S A* **85:**5240-5243.

Thompson CM, Capdevila JH and Strobel HW (2000) Recombinant cytochrome P450 2D18 metabolism of dopamine and arachidonic acid. *J Pharmacol Exp Ther* **294:**1120-1130.

Venn RF and Michalkiewicz A (1990) Fast reliable assay for morphine and its metabolites using high-performance liquid chromatography and native fluorescence detection. *J Chromatogr* **525:**379-388.

Voirol P, Jonzier-Perey M, Porchet F, Reymond MJ, Janzer RC, Bouras C, Strobel HW, Kosel M, Eap CB and Baumann P (2000) Cytochrome P-450 activities in human and rat brain microsomes. *Brain Res* **855:**235-243.

Wolkenstein P, Tan C, Lecoeur S, Wechsler J, Garcia-Martin N, Charue D, Bagot M and Beaune P (1998) Covalent binding of carbamazepine reactive metabolites to P450 isoforms present in the skin. *Chem Biol Interact* **113:**39-50.

Yu A, Dong H, Lang D and Haining RL (2001) Characterization of dextromethorphan O- and N-demethylation catalyzed by highly purified recombinant human CYP2D6. *Drug Metab Dispos* **29:**1362-1365.

Yu A and Haining RL (2001) Comparative contribution to dextromethorphan metabolism by cytochrome P450 isoforms in vitro: can dextromethorphan be used as a dual probe for both CTP2D6 and CYP3A activities? *Drug Metab Dispos* **29:**1514-1520.

Yu A, Kneller BM, Rettie AE and Haining RL (2002) Expression, purification, biochemical characterization, and comparative function of human cytochrome P450 2D6.1, 2D6.2, 2D6.10, and 2D6.17 allelic isoforms. *J Pharmacol Exp Ther* **303:**1291-1300.

Yu AM, Idle JR, Herraiz T, Kupfer A and Gonzalez FJ (2003) Screening for endogenous substrates reveals that CYP2D6 is a 5-methoxyindolethylamine O-demethylase. *Pharmacogenetics* **13:**307-319.

Yue QY and Sawe J (1997) Different effects of inhibitors on the O- and N-demethylation of codeine in human liver microsomes. *Eur J Clin Pharmacol* **52:**41-47.

Footnotes

This work supported in part by grant ES09894 from the NIEHS

Address reprint requests to:

Robert L. Haining, Ph. D

Department of Basic Pharmaceutical Sciences

School of Pharmacy

West Virginia University

PO Box 9530

Morgantown, WV 26506-9530

Tel: (304) 293-1450

Fax: (304) 293-2576

Email: rhaining@hsc.wvu.edu

Figure Legends

Figure 1. SDS-PAGE analysis of various fractions during the purification of hexa-histidine tagged mouse Cyp2d22 (HT-Cyp2d22). A resolving gel polymerized from 9% acrylamide was used to separate proteins using a standard TBE buffer system followed by staining with Coomassie blue. Lane 1: Membrane preparation from *T. ni* culture expressing HT-Cyp2d22. Lane 2: Flow-through from Ni-NTA Superflow during loading. Lane 3: Pooled fractions with wash buffer A. Lane 4: Pooled fractions with wash buffer B. Lane 5: Pooled fractions with wash buffer C. Lane 6: Final purified HT-Cyp2d22. Lane 7: Final purified HT-CYP2D6 by following the same protocol. Lane 8: Final purified non-polyhistidine-tagged CYP2D6 (Yu et al., 2001). Lane 9: Molecular weight markers in descending order: phosphorylase b, 97.4 kDa; bovine serum albumin, 68.0 kDa; ovalbumin, 43.0 kDa; carbonic anhydrase, 29.0 kDa; lysozyme, 14.3 kDa.

Figure 2. Typical CO difference spectrum of mouse HT-Cyp2d22 showing the maximal absorbance at 449 nm. Standard procedures (Omura and Sato, 1964) were followed.

Figure 3. Michaelis-Menten saturation curves for dextromethorphan O-demethylation (panel A) and N-demethylation (panel B) as catalyzed by recombinant Cyp2d22. Purified Cyp2d22 was reconstituted with lipid and rat cytochrome P450-reductase as described in Methods prior to initiation.

Figure 4. Michaelis-Menten saturation curves for codeine N-demethylation (panel A), fluoxetine N-demethylation (panel B), and methadone N-demethylation (panel C) as catalyzed by recombinant Cyp2d22.

Figure 5. Alignment of the amino acid sequence of mouse CYP2D22 to human CYP2D6 and CYP3A4 proteins.

Table 1. Estimated kinetic parameters for dextromethorphan *O*- and *N*-demethylation catalyzed by CYP2D6, HT-CYP2D6, HT-Cyp2d22 and CYP3A4 isozymes. Each data point used to calculate kinetic constants was based on an average of duplicate determinations. Enzyme Michaelis-Menten parameters and error estimates thereof were generated by nonlinear regression analysis (GraphPad Prizm 3.02)

Reaction	P450 isoform	V_{max} pmol/pmol P450/min	K_m μM	V_{max}/K_m nL/pmol P450/min
Dextromethorphan *O*-demethylation	CYP2D6	13.9 ± 0.4	5.1 ± 0.7	2700
	HT-CYP2D6	7.8 ± 0.4	4.2 ± 0.7	1900
	HT-Cyp2d22	7.7 ± 0.4	250 ± 30	31
	CYP3A4	5.6 ± 0.1	170 ± 10	33
Dextromethorphan *N*-demethylation	CYP2D6	55.3 ± 15.8	3900 ± 1700	14
	HT-CYP2D6	69.7 ± 6.6	4800 ± 900	15
	HT-Cyp2d22	20.4 ± 1.3	420 ± 60	49
	CYP3A4	24.5 ± 0.4	300 ± 20	81

Table 2. Calculated kinetic parameters for codeine, fluoxetine and methadone biotransformations catalyzed by CYP2D6, HT-CYP2D6, HT-Cyp2d22 and CYP3A4 isoforms. Each data point used to calculate kinetic constants was based on an average of duplicate determinations. Enzyme Michaelis-Menten parameters and error estimates thereof were generated by nonlinear regression analysis (GraphPad Prizm 3.02)

Reaction	P450 isoform	Vmax pmol/pmol P450/min	Km μM	Vmax/Km nL/pmol P450/min
Codeine *O*-demethylation	CYP2D6	6.3 ± 0.3	180 ± 33	35
	HT-CYP2D6	3.7 ± 0.2	280 ± 44	13
	HT-Cyp2d22		ND	
	CYP3A4		ND	
Codeine *N*-demethylation	CYP2D6		ND	
	HT-CYP2D6		ND	
	HT-Cyp2d22	3.8 ± 0.3	2200 ± 500	1.8
	CYP3A4	50 ± 1	620 ± 44	81
Fluoxetine *N*-demethylation	CYP2D6	0.53 ± 0.05	6.6 ± 1.3	84
	HT-CYP2D6	0.38 ± 0.01	2.5 ± 0.2	150
	HT-Cyp2d22	0.75 ± 0.08	110 ± 29	6.8
	CYP3A4	0.20 ± 0.11	170 ± 24	1.2
Methadone *N*-demethylation	CYP2D6		ND	
	HT-CYP2D6		ND	
	HT-Cyp2d22	4.9 ± 0.5	520 ± 100	9.5
	CYP3A4	3.5 ± 0.01	33 ± 6	110

ND: Not Detectable

Figure 1:

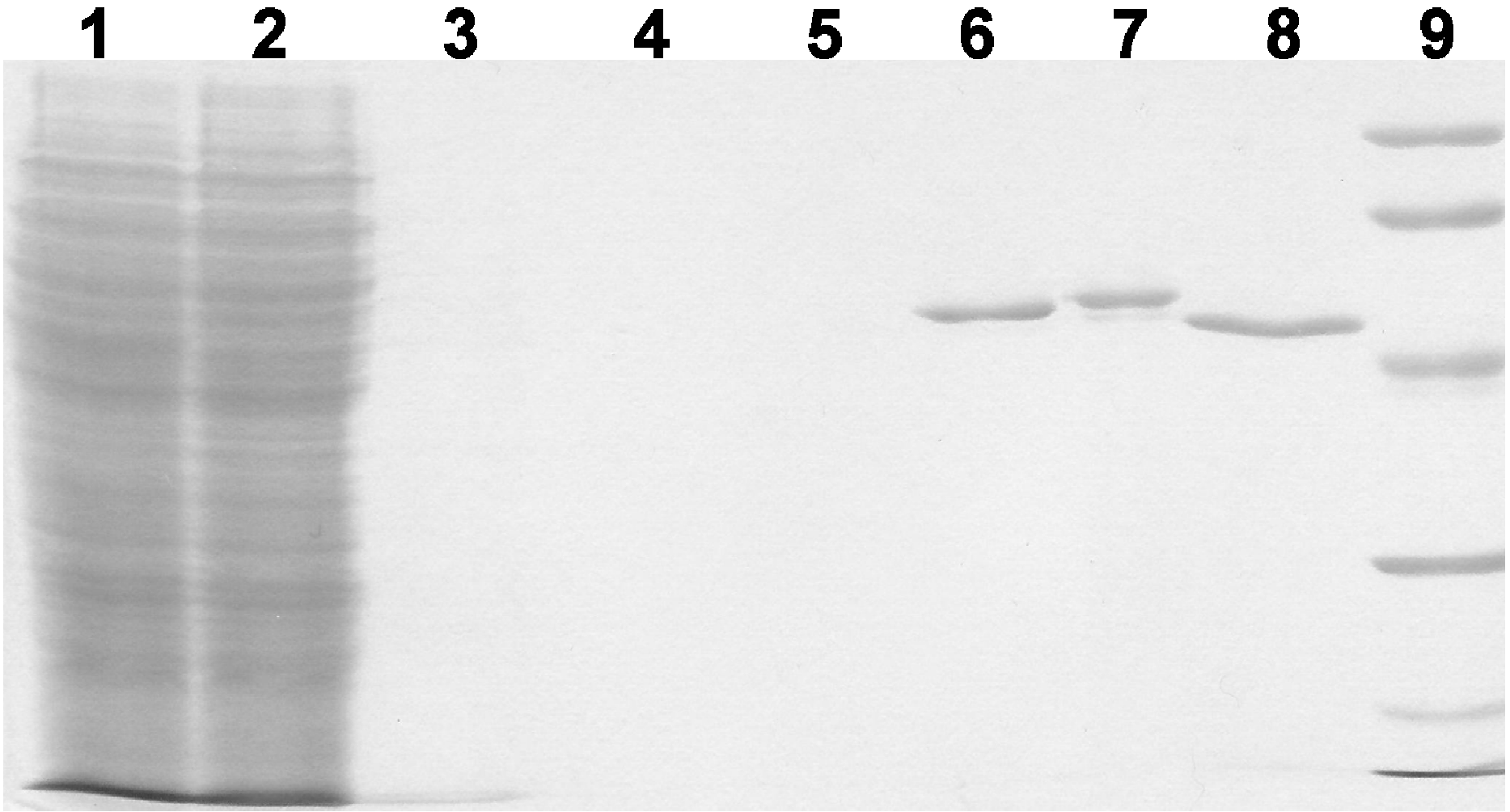

Figure 2:

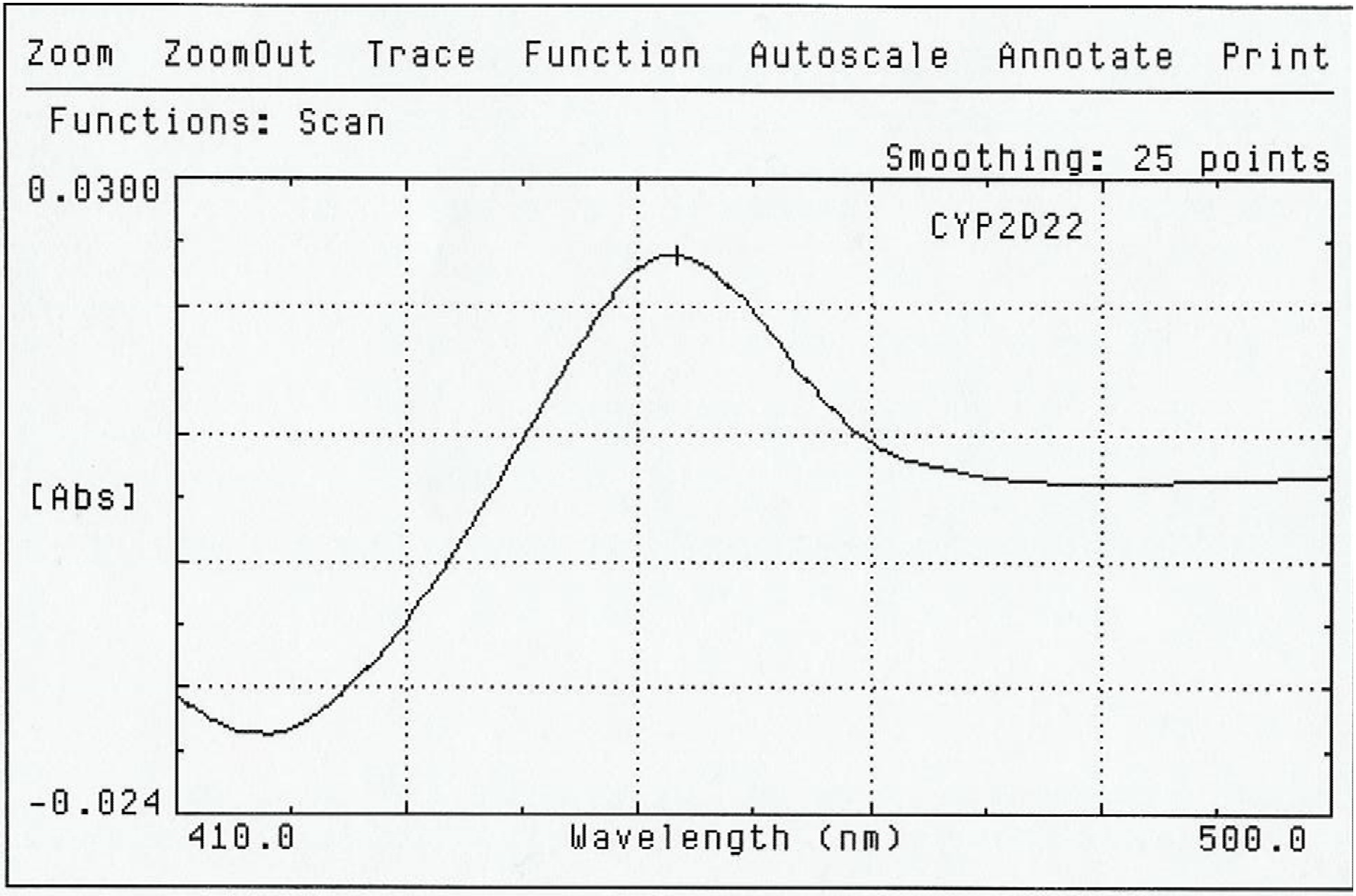

Figure 3:

A.

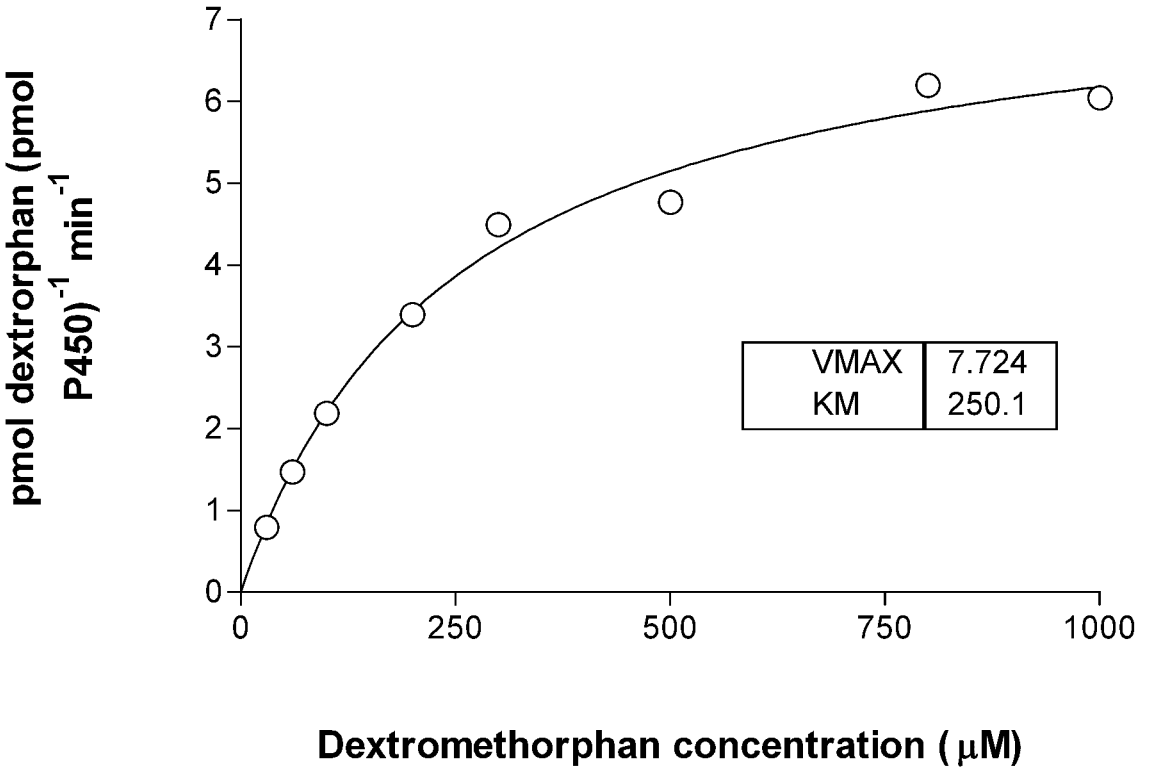
pmol dextrorphan (pmol P450)-1 min-1
0
1
2
3
4
5
6
7
0
250
500
750
1000
VMAX 7.724
KM 250.1
Dextromethorphan concentration (μM)

B.

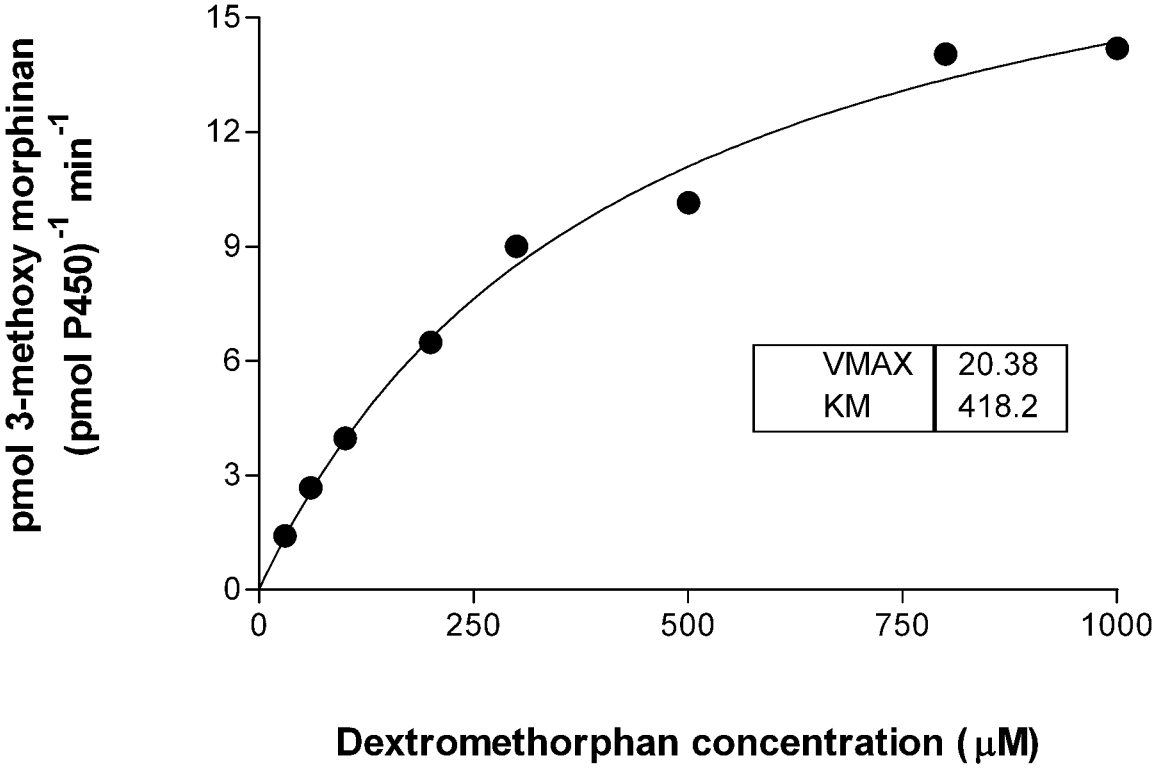
pmol 3-methoxy morphinan (pmol P450)-1 min-1
0
3
6
9
12
15
0
250
500
750
1000
VMAX 20.38
KM 418.2
Dextromethorphan concentration (μM)

Figure 4:

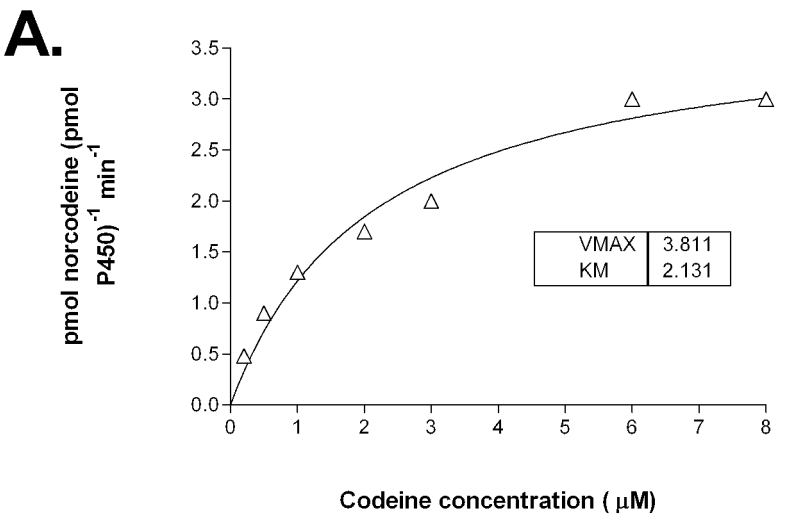
A.
pmol norcodeine (pmol P450)-1 min-1
3.5
3.0
2.5
2.0
1.5
1.0
0.5
0.0
0
1
2
3
4
5
6
7
8
VMAX 3.811
KM 2.131
Codeine concentration (μM)

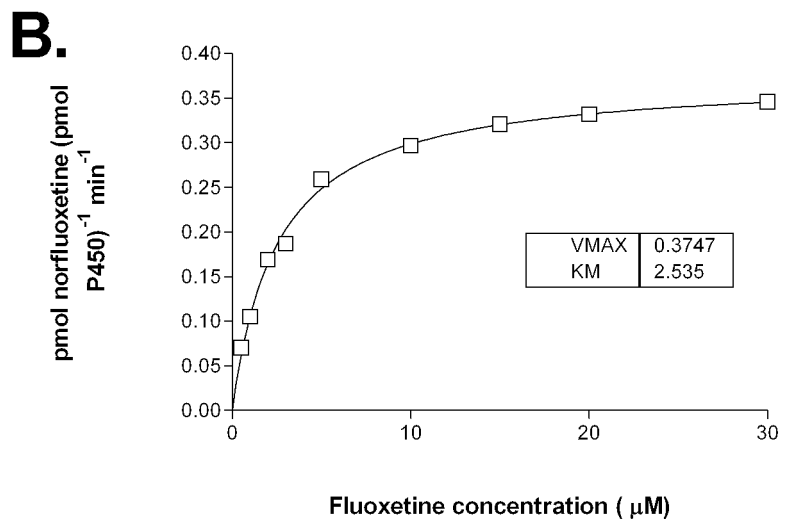
B.
pmol norfluoxetine (pmol P450)-1 min-1
0.40
0.35
0.30
0.25
0.20
0.15
0.10
0.05
0.00
0
10
20
30
VMAX 0.3747
KM 2.535
Fluoxetine concentration (μM)

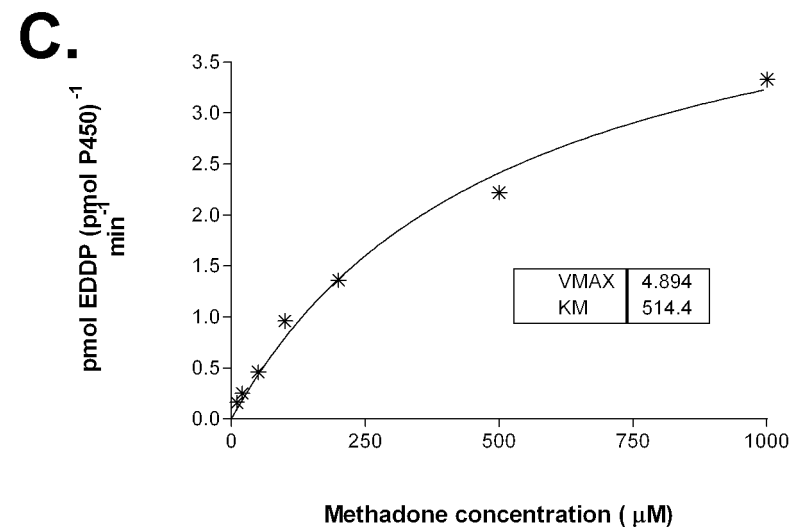
C.
pmol EDDP (pmol P450)-1 min-1
3.5
3.0
2.5
2.0
1.5
1.0
0.5
0.0
0
250
500
750
1000
VMAX 4.894
KM 514.4
Methadone concentration (μM)

Figure 5: